Effect of frustration near the magnetic-nonmagnetic transition

M. D. Núñez Regueiro,* C. Lacroix, and R. Ballou
Laboratoire Louis Neél, Centre National de la Recherche Scientifique, Boîte Postale 166, 38042 Grenoble CEDEX 9, France
(Received 26 December 1991)

Many different physical situations can be explained by the effect of frustration in systems close to the magnetic instability. We study this phenomenon within a Blume-Capel model on a triangular lattice, by numerical and analytical calculations. Complex magnetic ordered phases, including coexistence of magnetic and nonmagnetic sites, are obtained. The interesting dependence of the phase diagram with pressure, magnetic field, and temperature is discussed in connection with experimental results on $R\mathrm{Mn}_2$ systems.

I. INTRODUCTION

Frustration is frequently present in magnetic systems and its consequences on the physical properties are under active discussion in the literature. The spin-glass behavior is the result of frustration in disordered systems. Frustration also occurs in both metallic and insulating periodic systems, either because it is inherent to the crystal structure, or due to competing interactions. The low-temperature behavior of such systems is very rich because of the existence of many states with similar energies. In rare-earth metals helimagnetic (Tb, Dy) and antiphase (Tm) orderings have been recognized for a long time. More recently other exotic behaviors have been reported: $Gd_3Ga_5O_{12}$ does not order even at low temperature;[1] spin-nematic order has been proposed for the Heisenberg antiferromagnet on a Kagomé lattice: $SrCr_8Ga_4O_{19}$.[2] In another context, frustration certainly plays a role when cuprate perovskites are doped.[3]

In all the previous cases all relevant sites are magnetic. In a recent work,[4] however, in order to explain the peculiar properties of itinerant antiferromagnetic (AF) $R\mathrm{Mn}_2$ (R denotes rare earth) systems, another possibility has been considered: the instability of the magnetic moment. Frustration near the magnetic-nonmagnetic (M-NM) transition yields complex magnetic ordered phases in which magnetic and nonmagnetic sites coexist and which show unusual dependence on external parameters such as magnetic field, temperature, applied pressure, or alloying. This is in fact a more general phenomenon: a similar situation can occur in frustrated Ce compounds where the nonmagnetic state is attained by means of the Kondo effect or in compounds where the lowest crystal field level is a singlet.

We have then proposed[4] to map all these cases, near the M-NM transition, into a Blume[5]-Capel[6] model:

$$H=\sum_i \Delta S_i^2+\tfrac{1}{2}\sum_{i\neq j} J_{ij}S_iS_j \ , \tag{1}$$

where Δ and J_{ij} are related to the parameters of the microscopic model corresponding to the particular case. Close to the M-NM instability, $\Delta>0$ and S_i can take three values: $S_i=\pm 1$ if the site has a magnetic moment $\mu_i=\pm\mu$, and $S_i=0$ if $\mu_i=0$. This last choice breaks the rotational invariance of the spins, which is just the case of the $R\mathrm{Mn}_2$ systems where the Mn atoms are located on a site of high uniaxial symmetry.[7] The model can be improved by taking into account longitudinal as well as transverse fluctuations. In other cases it is necessary to consider from the beginning xy or Heisenberg interactions.

The frustration of the structure is described in a triangular lattice where it is not possible to satisfy all the AF nearest-neighbor interactions. Consider the triangle in Fig. 1. If the energy Δ necessary to create a moment is positive, configuration (b) has a lower energy than configuration (a). Thus on a triangular lattice the magnetic moments on some sites can vanish due to frustration. The same occurs in the more complicated Laves phase structure of the $R\mathrm{Mn}_2$ systems or in the Ce compounds with competing interactions.

The paper is organized as follows. In Sec. II we discuss different physical situations that lead to this interplay between instability of the magnetic moment and frustration. In Sec. III we describe the two methods used to study the Hamiltonian that we propose to model this phenomenon in Eq. (1). In Sec. IV we obtain the corresponding phase diagram on the triangular lattice at $T=0$ and $H=0$; its evolution with pressure is discussed. The magnetic field and temperature dependences are discussed in Secs. V and VI, respectively. Section VII contains the conclusions and some comments on experiments.

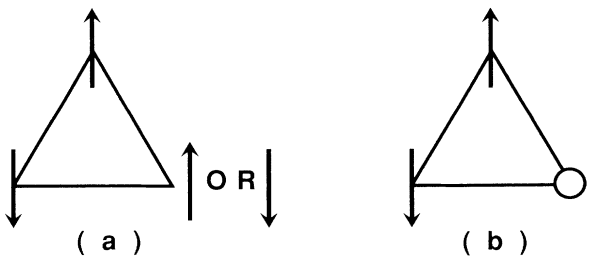

FIG. 1. Competing three-site configurations. (a) Three magnetic sites with total energy $E_T=3\Delta-J_1$. (b) Two magnetic sites with $E_T=2\Delta-J_1$ (○ indicates nonmagnetic site).

II. SOME PHYSICAL REALIZATIONS OF THE MODEL

A. RMn_2 compounds

The intermetallic RMn_2 compounds show interesting properties that are associated with the instability of the itinerant-electron antiferromagnetism in a frustrated lattice.

These compounds crystallize in either the $C14$ hexagonal or $C15$ cubic Laves phase structure. The Mn atoms occupy the corner of regular tetrahedra,[8] giving rise in both cases to a highly frustrated lattice. On the other hand, the Mn moments in the RMn_2 series are very close to the M-NM instability. Below a critical Mn-Mn distance d_c, Mn remains nonmagnetic, i.e, for R =Sc, Ho, Er, Tm, and Lu. Above d_c, i.e., with light lanthanides, R =Pr, Nd, Sm, and Gd, large moments with AF interactions are found.[9] Complex magnetic orderings are then observed due to the lattice frustration. They set in a first-order transition accompanied by a large volume discontinuity[9] which is accounted for by a substantial jump of the Mn moment at the ordering. In the compounds with a Mn-Mn spacing near d_c the magnetism becomes extremely sensitive to external parameters. A good illustration is $TbMn_2$. In the paramagnetic regime this compound exhibits strong short-range order. As the temperature is decreased two close magnetic transitions develop. At low temperature, the magnetic structure can be destabilized by an applied field, leading to magnetic isotherms with large field hysteresis.[10] Application of hydrostatic pressure induces a dramatic decrease of the ordering temperature of the Mn ions, at a rate of 36 K/kbar.[11] The substitution of only 3% of Tb by Sc is enough to destroy the Mn moment.[12] The case of $DyMn_2$ is particularly interesting, as although all the Mn sites are chemically equivalent, only 25% of them bear a magnetic moment. This coexistence of magnetic and nonmagnetic Mn sites has been clearly established by NMR (Ref. 13) and by powder neutron diffraction.[14]

In the RMn_2 compounds in which a Mn ordering takes place the Néel temperature is roughly independent of the rare earth R ($T_N \sim 100$ K).[8,9] This shows that the R-R and R-Mn exchange interactions are 1 order of magnitude smaller than the Mn-Mn interactions: we neglect them. We use for the Mn lattice a Hamiltonian derived from the Hubbard model close to the M-NM instability.

Using the functional-integral technique, the partition function of the Hubbard Hamiltonian can be written as an integral over N auxiliary variables μ_i (in the static approximation):[15]

$$Z=\int d\mu_i \exp[-\beta F(\mu_i)] , \tag{2}$$

where

$$F(\mu_i)=F_0-\frac{1}{\beta}\mathrm{Tr}\ln(1-VG_0)+\sum_i \frac{U\mu_i^2}{4} . \tag{3}$$

In this expression F_0 and the Green's function G_0 are related to the noninteracting part of the Hamiltonian,

$$H_0=\sum_{k,\sigma} \varepsilon_k c_{k\sigma}^{\dagger} c_{k\sigma} \tag{4}$$

and V is a nonuniform potential,

$$V=-\tfrac{1}{2}U\sum_i \mu_i(n_{i\uparrow}-n_{i\downarrow}) . \tag{5}$$

At zero temperature, the integral over μ_i in Eq. (2) is usually replaced by a saddle-point approximation. The auxiliary variables μ_i are determined by minimizing $F(\mu_i)$ and this is equivalent to a local Hartree-Fock approximation: $\mu_i=\langle n_{i\uparrow}-n_{i\downarrow}\rangle$.

It has been shown[15,16] that the main contributions to F come from the one-site $F_1(\mu_i^2)$ and two-site $F_2(\mu_i\mu_j)$ terms. Two situations can occur: (i) F_1 is minimum for $\mu_i=\pm\mu$ ($\mu\neq 0$). In this case all sites are magnetic and the ground state can be ordered due to the magnetic exchange energy [i.e., $F_2(\mu_i\mu_j)$]. This is the case for U larger than a critical value. (ii) F_1 is minimum for $\mu_i=0$. A magnetic moment can exist only if the two-site interactions are large enough. This occurs close to the M-NM transition.

F_1 and F_2 can be calculated numerically for a given band structure.[16] For small values of μ_i the following expressions for F_1 and F_2 can be derived from Eq. (3):[17]

$$F_1=\sum_i \tilde{\Delta}\mu_i^2 , \quad F_2=\tfrac{1}{2}\sum_{i\neq j} \tilde{J}_{ij}\mu_i\mu_j , \tag{6}$$

with

$$\tilde{\Delta}=\frac{U}{4}\left[1+\frac{U}{N}\sum_{k,q}\frac{f(\varepsilon_k)-f(\varepsilon_{k+q})}{\varepsilon_k-\varepsilon_{k+q}}\right] , \tag{7}$$

$$\tilde{J}_{ij}=\frac{U^2}{4N}\sum_{k,q} e^{iq(R_i-R_j)}\frac{f(\varepsilon_k)-f(\varepsilon_{k+q})}{\varepsilon_k-\varepsilon_{k+q}} . \tag{8}$$

$\tilde{\Delta}<0$ in case (i) and $\tilde{\Delta}>0$ in case (ii) above. In the following we suppose that $\tilde{\Delta}>0$. The magnetic moment at a given site, μ_i, which minimizes F_1+F_2 will be different from zero only if the molecular field around it is large enough to overcome the on-site energy $\tilde{\Delta}$. Thus we consider that μ_i can take three values, $\mu_i=0,\pm\mu$. This is the main difference from the earlier calculations where magnetic moments were supposed to have only two values, $\pm\mu$. Of course, for finite values of μ_i other contributions to F_1 and F_2 must be taken into account. However, the saddle-point approximation yields the same type of expression (6) (only the coefficients $\tilde{\Delta}$ and $\tilde{J}_{ij}$ are changed).

Equation (2) is then equivalent to the partition function of the spin Hamiltonian in Eq. (1), with

$$\Delta=\tilde{\Delta}\mu^2 , \quad J_{ij}=\tilde{J}_{ij}\mu^2 , \quad \text{and } S_i=0,\pm 1 . \tag{9}$$

This $S=1$ Ising-like model is particularly well suited for the RMn_2 compounds where the Mn lattice is submitted to a large uniaxial anisotropy.[7]

B. Kondo lattice compounds

Most of the Ce compounds that do not show magnetic ordering show, however, AF correlations at low temperature.[18] These correlations are induced by the Ruderman-

Kittel-Kasuya-Yosida (RKKY) interaction. In a lattice with such long-range interactions, frustration generally occurs because it is not possible to satisfy all AF correlations. This frustration will favor the Kondo effect: if a site is strongly frustrated it will be energetically more convenient to stabilize a singlet on that site. The Kondo lattice can then also be mapped on the effective Hamiltonian in Eq. (1). However, in this case

$$\Delta=\sum_q\left[\frac{1}{\chi_{ff}^{(0)}(q)}-J^2\chi_{cc}^{(0)}(q)\right], \tag{10}$$

$$J_{ij}=-\sum_q e^{iq(R_i-R_j)}\left[\frac{1}{\chi_{ff}^{(0)}(q)}-J^2\chi_{cc}^{(0)}(q)\right], \tag{11}$$

are related to the localized and conduction-band Kondo susceptibilities in the nonmagnetic state[19] $\chi_{ff}^{(0)}$ and $\chi_{cc}^{(0)}$, and they depend on temperature.

Experimental indications for this behavior are the metamagnetic transitions induced by the application of a magnetic field in $CeRu_2Si_2$, for example.[20] Also CeSb where magnetic planes alternate with nonmagnetic planes[21] could be analogous to the mixed phase observed in RMn_2 systems.

C. Crystal field effects

The same kind of Hamiltonian in Eq. (1) was first proposed by Blume[5] and Capel[6] for the following case: the ground state of a system is a singlet and a magnetic level lies at an energy Δ above the singlet. In a magnetic field the magnetic level is split while the singlet remains unaffected. If the magnetic field is large enough, the ground state will have a net magnetic moment. If the magnetic field is smaller than $\Delta/g\mu_B$, however, the system will be nonmagnetic. The same happens if the magnetic field is due to exchange interactions between the various ions, and if frustration is present one or the other situation can occur on sites that are chemically equivalent. This is the case of $TbNi_2Si_2$ (Ref. 22) and $PrNi_2Si_2$ (Ref. 23) where this effect gives rise to incommensurate modulated structures down to $T=0$ K.[24]

D. Dense classical Coulomb gas

A similar model has recently been proposed for the classical Coulomb gas of integer charges on a triangular lattice and related problems: superfluid and superconducting films, Josephson-junction arrays, two-dimensional (2D) melting surface roughening and liquid crystals. In spite of the fact that the interaction is long range and the interest is focused on the 2D properties, the phase diagram reported by Lee and Teitel[25] shows many similarities with our work. Particularly these authors also obtain the mixed phase (phase VI in Fig. 2), with simultaneous charged and neutral sites: $q_i=\pm q$ or 0.

III. METHODS

We propose then to map all the previous cases on the effective spin model in Eq. (1). We have studied this Hamiltonian for temperature-independent parameters Δ and J_{ij} which could correspond to the cases described in Secs. II A, II C, and II D, but not to the one described in Sec. II B, by numerical and analytical calculations.

For the general case there are no exact results. In the limit $\Delta\rightarrow-\infty$, nearest-neighbor interaction $J_1>0$ and next-nearest and third-neighbor interactions, $J_2=J_3=0$, Eq. (1) is equivalent to the AF $S=\frac{1}{2}$ Ising model, which in the triangular lattice does not order: the simultaneous reversal of pairs of spins does not cost any energy.[26] The molecular field calculations and the Monte Carlo simulations with periodic boundary conditions do not reproduce this result. However, we are interested in the case $\Delta>0$ for which no exact results are known. As is shown in the next section, for $J_2=J_3=0$ the stable phase is a mixed one with coexistence of magnetic and nonmagnetic sites (see phase VI in Fig. 5), for which the previous argument is no longer valid: it is not possible to reverse spins without increasing the energy. On the other hand, the magnetic phases are obtained for J_2 or $J_3\neq0$ where this argument also cannot be applied.

We have used two different methods to study Eq. (1) and we have verified in all cases agreement of the results

(a) Monte Carlo simulations using Metropolis sampling on 10×12, 12×12 *and* 16×12 *lattices with periodic boundary conditions.* Some simulations have also been performed with free boundary conditions in order to check that no other structures with different periodicity are stabilized.

(b) Analytical calculations where correlations in the elementary magnetic cell are treated exactly. For example, for a three-site unit cell, the partition function Z is evaluated replacing the Hamiltonian in Eq. (1) by

$$H^P=H_0^P+V^P, \tag{12}$$

$$H_0^P=J_1(S_1S_2+S_2S_3+S_1S_3)+\Delta(S_1^2+S_2^2+S_3^2), \tag{13}$$

$$V^P=\sum_{i=1}^{3}V_i^PS_i \quad\text{with } V_i^P=\sum_j{}'J_{ij}m_j \quad\text{for } j\neq1,2,3, \tag{14}$$

where the sites 1, 2, and 3 form a triangle. V^P represents the interaction with the other sites which is treated in mean field approximation. $\sum'$ includes all other sites except 1, 2, and 3. The advantage of this second method is that analytical results can be obtained, where frustration is partially taken into account. The magnetic moments are calculated self-consistently:

$$m_i^P=\frac{\sum_{(c)}S_i^{(c)}e^{-\beta H^P}}{\sum_{(c)}e^{-\beta H^P}}=\frac{A_i^P}{Z^P}, \tag{15}$$

where (c) means the different possible configurations for the three sites merged in the studied phase P. The comparison of the free energies corresponding to the different phases:

$$F^P=-kT\ln Z^P-\tfrac{1}{2}\sum_{i=1}^{3}{}'\sum_j{}'\langle m_i^P\rangle\langle m_j^P\rangle \quad\text{with } j\neq1,2,3 \tag{16}$$

allows one to study the temperature dependence of the phase diagram, discussed in Sec. VI.

IV. PHASE DIAGRAM AT $T=0$ AND $H=0$

The two methods described before lead to the same phase diagram for the model Hamiltonian in Eq. (1) at low temperatures. Although many other configurations have been taken into account, only the ordered structures plotted in Fig. 2 have been stabilized at zero field in the range of parameters considered. If the on-site energy Δ and the interactions J_{ij} are related to the parameters of the Hubbard model, we can think that Δ increases considerably with the application of pressure while the J_{ij} interactions change but in a more moderate way. Figure 3 shows the evolution of the $T=0$, $H=0$ phase diagram with Δ when first-, second-, and third-neighbor interactions are included. Preliminary results have been given elsewhere.[27]

For $\Delta=0$ all phases are magnetic [Fig. 3(a)]. For finite Δ an ordered phase in which magnetic and nonmagnetic sites coexist appears for $|J_2|<\Delta/3$ [Fig. 3(b)]. This new mixed phase VI (hexagons of alternating up and down spins with a nonmagnetic sites at the center) is stabilized between the ferrimagnetic phase III (hexagons of up spins with a down spin at the center) and the AF phase IV (zigzag up and zigzag down spin chains). For increasing Δ ($\Delta/J_1>\frac{3}{2}$) this last phase, IV, disappears and a new mixed ordered one, VII, is stabilized (zigzag up and zigzag down chains alternate but leaving a nonmagnetic site at the center of the hexagons that they form) [Fig. 3(c)]. A third, more complicated mixed phase VIII appears for larger Δ and larger interactions J_{ij} [Fig. 3(d)]. For Δ very large it is energetically more convenient to cancel moments and the nonmagnetic phase IX spreads over the

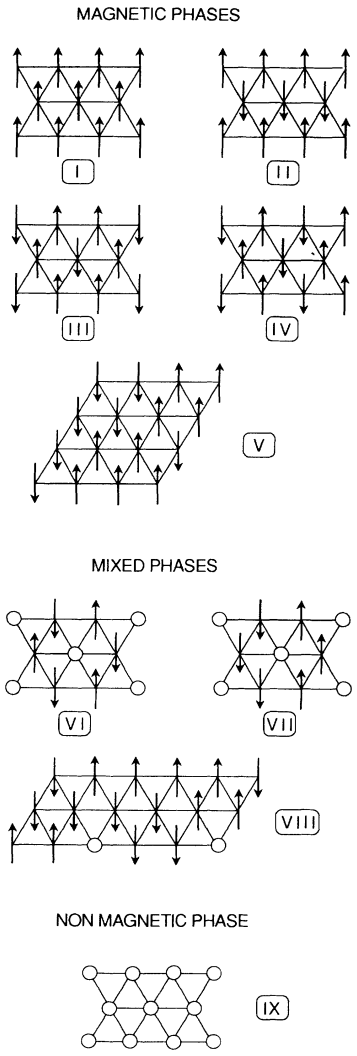

FIG. 2. Ordered phases stabilized in the range of parameters considered in Fig. 3. In the text the different phases are referred to using the numbers indicated in this figure.

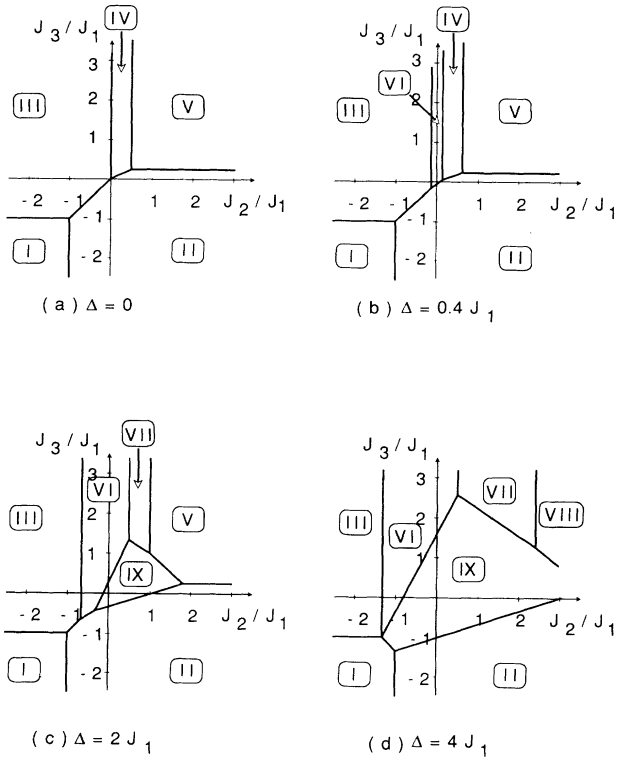

FIG. 3. Phase diagram of the model Hamiltonian [Eq. (1)], on the triangular lattice at $T=0$, $H=0$, with increasing on-site energy Δ. The borderlines between the different phases defined in Fig. 2 are determined by the following equations: phases I and II, $J_1=-J_2$; phases I and III, $J_1=-J_3$; phases II and III, $J_2=J_3$; phases II and IV, $J_2=2J_3$; phases III and IV, $J_2=0$; phases II and V, $J_1=4J_3$; phases IV and V, $J_1=2J_2$; phases II and VI, $\Delta=9J_2-12J_3$; phases III and VI, $\Delta=-3J_2$; phases IV and VI, $\Delta=3J_2$; phases V and VII, $\Delta=J_1+J_2$; phases VI and VII, $J_1=2J_2$; phases II and IX, $\Delta=J_1+J_2-3J_3$; phases V and IX, $\Delta=J_2+J_3$; phases VI and IX, $2\Delta=3J_1-6J_2+3J_3$; phases VII and IX, $2\Delta=-J_1+2J_2+3J_3$; phases VII and VIII, $2\Delta=3J_2$; phases VIII and IX, $8\Delta=-3J_1+9(J_2+J_3)$.

magnetic and mixed phases [Fig. 3(d)].

The phases obtained can be classified in three categories which can be related to different $R\mathrm{Mn}_2$ compounds, depending on the Mn-Mn distance.

(I)–(V) magnetic phases (YMn_2, $NdMn_2$). When $|S_i|=1$ on each site, different magnetic orderings can be obtained, depending on the J_2/J_1 and J_3/J_1 ratios. The evolution of each of these phases with Δ (i.e., with increasing pressure) is different: in some cases the magnetism is canceled homogeneously, whereas for other parameters only partial vanishing occurs and mixed phases are obtained.

(VI)–(VIII) mixed magnetic phases ($ThMn_2$, $DyMn_2$). These phases are new and occur in compounds with Mn-Mn distance $d \sim d_c$ or, for special ratios of the parameters which are attained by modifying the external conditions: temperature, magnetic field ($TbMn_2$ below 40 K at $H>4.5$ T,[28] see Sec. V), pressure ($TbMn_2$ at $P>2$ kbar).[29] NMR measurements have determined unambiguously this behavior, neutron diffraction experiments have been done to determine the arrangement of the magnetic and nonmagnetic sites.

(IX) nonmagnetic phase ($ScMn_2$, $ErMn_2$). For large Δ, $S_i=0$ at each Mn site.

Since all these phases are observed with either magnetic (Er, Nd, Dy) or nonmagnetic (Sc, Y, Th) rare earths, they are characteristic solely of the Mn lattice.

V. MAGNETIC FIELD DEPENDENCE

The effect of an applied field is interesting: several transitions are induced, their number depending on the initial state in zero field. Furthermore, Monte Carlo simulations show an unexpected feature: at some critical fields the number of magnetic sites decreases with increasing field. Figure 4 shows the evolution of an AF initial state ($\Delta=J_1$, $J_2=J_1/2$, and $J_3=0$): four transitions are observed at $h_1=-\Delta+2(J_1+J_2)$, $h_2=\Delta+2(J_1+J_2)$, $h_3=-\Delta+6(J_1+J_2)$, $h_4=\Delta+6(J_1+J_2)$. Above the first and the third critical fields new mixed phases are obtained, which were not stabilized without field.

According to recent neutron diffraction experiments this behavior occurs in $TbMn_2$.[28] With a magnetic field this compound, initially in an AF state, tips over a mixed phase, where Mn magnetic moments coexist with 75% of nonmagnetic Mn sites in the more complicated Laves phase structure.[28] By cooling this compound under applied field and returning to zero field, a different ordered state is obtained, showing another characteristic of frustrated lattices: many different phases are very close in energy.

VI. TEMPERATURE DEPENDENCE

A systematic study of the phase diagram with the analytical method explained in Sec. III shows that the temperature behavior is also very rich, with first- and second-order as well as multiple transitions, depending on the parameter values. In Fig. 5 we indicate the regions where these different behaviors are observed for first- and second-neighbor interactions ($J_3=0$). In this case the competing ordered states are described below.

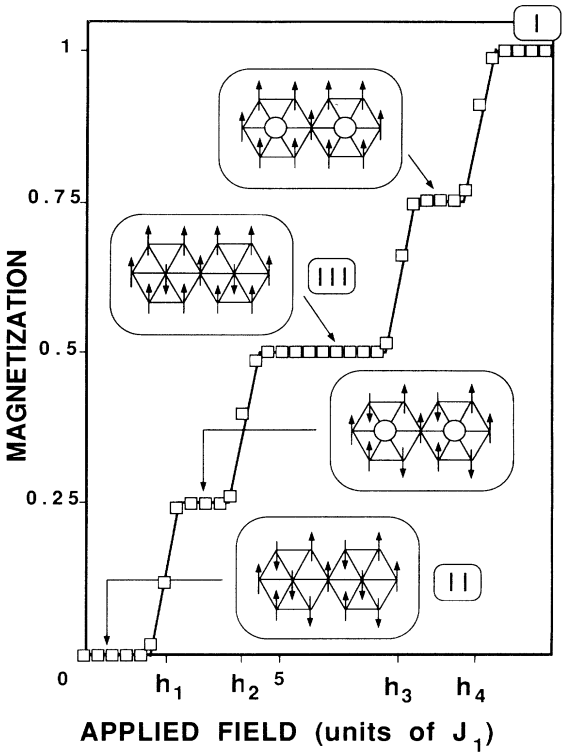

FIG. 4. Monte Carlo simulation for increasing magnetic field, for $\Delta=J_1$ and $J_2=J_1/2$, corresponding to the antiferromagnetic phase II in zero field. Two additional mixed phases are obtained.

(a) The mixed phase VI, for which the elementary magnetic cell is a triangle with $m_i^M=\langle S_i^M\rangle=0,\pm m^M$, yielding

$$V^M=\tilde{J}m^M(S_2-S_1)\ , \tag{17}$$

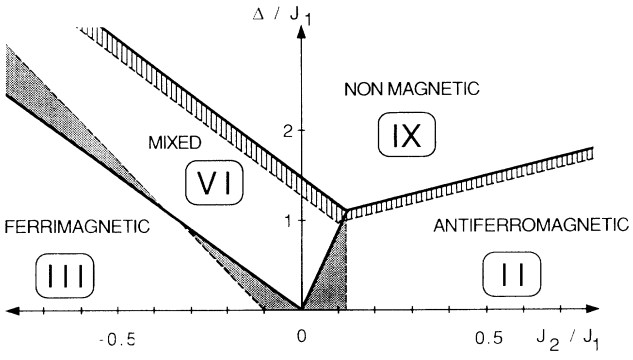

FIG. 5. Phase diagram for first- and second-neighbor interactions, $J_3=0$. The solid lines indicate the phase boundaries at $T=0$. The dashed lines separate regions with different temperature behavior: ▩ means that a first-order transition from the ground state to another ordered state is observed at $T_{N'}$, before reaching the nonmagnetic state at T_N; ▥ indicate regions where the transition at T_N is first order. In the other part of the diagram the transition to the nonmagnetic state at T_N is second order.

where

$$\tilde{J}=2J_1-6J_2+3J_3 \ . \tag{18}$$

With this molecular field, following Eq. (15) we calculate

$$m_{\uparrow}^{M}=-m_{\downarrow}^{M}=m^{M}=\frac{A^{M}}{Z^{M}} \tag{19}$$

and the free energy per site is given by Eq. (16):

$$F^{M}=\tfrac{1}{3}\{-kT\ln Z^{M}+\tilde{J}(m^{M})^2\} \ . \tag{20}$$

(b) The ferrimagnetic phase III, where the triangular unit cell has $m_i^F=m_{\uparrow}^F$ or $m_{\downarrow}^F$, and

$$V^F=(\tilde{J}m_{\uparrow}^F-\tilde{\tilde{J}}m_{\downarrow}^F)(S_1+S_2)+(2\tilde{\tilde{J}}m_{\uparrow}^F-6J_2m_{\downarrow}^F)S_3 \ , \tag{21}$$

with

$$\begin{aligned}\tilde{J}&=2J_1+6J_2+3J_3 \ ,\\ \tilde{\tilde{J}}&=2J_1+3J_3 \ ,\end{aligned} \tag{22}$$

and

$$m_{\uparrow}^F=\frac{A_{\uparrow}^F(m_{\uparrow}^F,m_{\downarrow}^F)}{Z^F(m_{\uparrow}^F,m_{\downarrow}^F)} \ , \quad m_{\downarrow}^F=\frac{A_{\downarrow}^F(m_{\uparrow}^F,m_{\downarrow}^F)}{Z^F(m_{\uparrow}^F,m_{\downarrow}^F)} \ . \tag{23}$$

In this case the self-consistency includes these two equations which verify the condition

$$\lim_{T\to T_N}\frac{m_{\uparrow}^F}{m_{\downarrow}^F}\to\tfrac{1}{2} \tag{24}$$

as can be easily by expanding Eqs. (23) for $m\to 0$. The free energy per site is given by

$$\begin{aligned}F^F=\tfrac{1}{3}[&-kT\ln Z^F-\tilde{J}(m_{\uparrow}^F)^2-3J_2(m_{\downarrow}^F)^2\\ &+2\tilde{\tilde{J}}(m_{\uparrow}^F)(m_{\downarrow}^F)] \ .\end{aligned} \tag{25}$$

(c) The AF phase II, for which the unitary magnetic cell contains only two sites, with $m_i=\pm m^A$. The molecular field Hamiltonian reads

$$H^A=J_1S_1S_2+\Delta(S_1^2+S_2^2)+\tilde{J}m^A(S_2-S_1) \ , \tag{26}$$

with

$$\tilde{J}=J_1+J_2-6J_3 \ . \tag{27}$$

In this case there is only one self-consistent equation:

$$m_{\uparrow}^A=-m_{\downarrow}^A=m^A=\frac{A^A(m^A)}{Z^A} \tag{28}$$

and the free energy per site is

$$F^A=\tfrac{1}{2}[-kT\ln Z^A+\tilde{J}(m^A)^2] \ . \tag{29}$$

The comparison of the free energies of these configurations indicates (see Fig. 5) that two successive transitions at $T_{N'}$ and T_N are obtained with increasing temperature near the borderline between the mixed phase VI and the ferrimagnetic phase III, $J_2=-\Delta/3$ (for $J_3=0$). For $\Delta>J_1$, the number of magnetic sites increases with temperature before having cancellation of the moment in all sites: at $T_{N'}$ one goes from phase VI to phase III before attaining the nonmagnetic states at T_N. This case is shown in Fig. 6. The opposite occurs for $\Delta<J_1$: with increasing temperature the magnitude of the up moments of the ferrimagnetic phase III decreases faster than the opposite component in order to attain the relation given in Eq. (24), but before arriving at the ratio of 1/2, a transition to the mixed phase VI occurs. The vanishing of the magnetic moment is done only in some sites before reaching the homogeneous nonmagnetic phase.

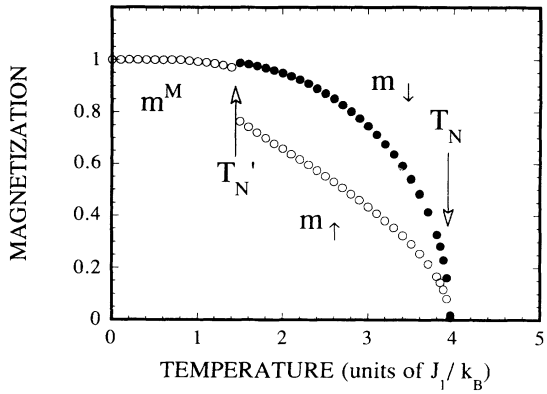

FIG. 6. Temperature dependence of the magnetic moments for $\Delta/J_1=2.5$ and $J_2/J_1=-0.8$, $J_3=0$. m^M is the amplitude of the magnetic moments in the mixed phase VI; $m_{\uparrow}^F$ and $m_{\downarrow}^F$ correspond to the ferrimagnetic phase III. Note that just below T_N, $m_{\uparrow}^F/m_{\downarrow}^F\to\frac{1}{2}$, verifying Eq. (24).

As a function of temperature, also Monte Carlo simulations indicate that several transitions take place for some values of the parameters J_{ij} and Δ, which are reflected in the thermodynamical properties. For the parameters of Fig. 6, at low temperature the ground state is the mixed phase VI but between $T_{N'}$ and T_N the ferrimagnetic phase III is stabilized in the simulations. The specific heat, plotted in Fig. 7, clearly shows the existence of these two transitions.

In order to understand these numerical results, we have performed high-temperature expansion, using the

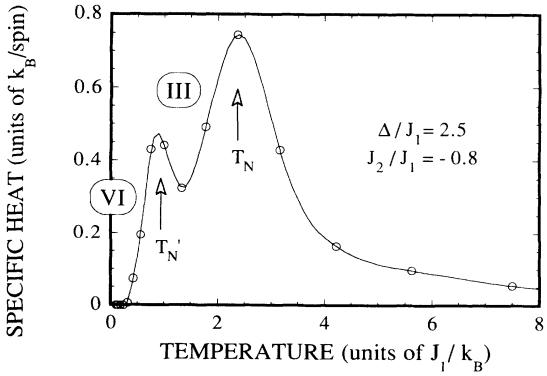

FIG. 7. Specific heat calculated by Monte Carlo simulations: $C_v=[\langle E^2\rangle-\langle E\rangle^2]/k_BT^2$ for the same parameters as in Fig. 6.

three-site mean field approximation described above. We find that the transition temperature T_N depends only on the q vector which characterizes the ordered state below T_N. If the transition is second order one has

$$k_B T_N(q) = -X[J(q) - J_1 f(q)] - Y[J(q) f(q) - J_1 f(q) - 2J_1] , \quad (30)$$

where

$$X = \mathrm{Tr}[S_1^2 \exp(-\beta H_0)] / \mathrm{Tr}[\exp(-\beta H_0)] , \quad (31)$$

$$Y = \mathrm{Tr}[S_1 S_2 \exp(-\beta H_0)] / \mathrm{Tr}[\exp(-\beta H_0)] , \quad (32)$$

$$f(q) = \frac{2}{3}\left[\cos q_x + \cos\left[\frac{q_x}{2} + \frac{\sqrt{3}}{2} q_y\right] + \cos\left[\frac{q_x}{2} - \frac{\sqrt{3}}{2} q_y\right]\right] . \quad (33)$$

$J(q)$ is the Fourier transform of J_{ij}. H_0 is given by Eq. (13).

The mixed phase VI corresponds to $q_1 = (2\pi/3, 2\pi/\sqrt{3})$, $J(q_1) = -3J_1 + 6J_2$. The antiferromagnetic phase II corresponds to $q_2 = (0, 2\pi/\sqrt{3})$ and $J(q_2) = -2J_1 - 2J_2$. The ferrimagnetic phase III is described by two different q values: q_1 and $q_0 = (0,0)$, $J(q_0) = 6J_1 + 6J_2$.

When the temperature decreases the stable phase is the one with the highest $T_N(q)$. However, phases VI and III have the same T_N, since they both correspond to the same $q = q_1$. Below T_N, in phase VI only one order parameter $m_q = \langle S_i \exp(iqR_i) \rangle$ is different from zero, whereas in phase III two order parameters, m_q and m_0 (uniform magnetization), must be considered. m_0 is much smaller than m_q, below T_N: $m_0 \sim |m_q|^3$ with $m_q \sim (T_N - T)^{1/2}$. Expansion of the free energy up to the sixth order in βV must be performed in order to find a difference between the two phases: $F^M - F^F \sim A(T_N - T)^3$ where the sign of A depends on the parameters. The results shown in Figs. 6 and 7 correspond to the case where A is positive: thus decreasing temperature below T_N, phase II has a lower energy than phase VI, but as phase VI is the stable one at $T = 0$ K, a second transition occurs at $T_{N'} < T_N$ between phases III and VI. This second transition is a first-order one with a discontinuity in the values of m_q and m_0. (The coefficient A can be calculated easily in the one-site mean field approximation and it is then found to be proportional to $J(q_0)$. This estimation gives a larger parameter region for the existence of two transitions: $J_2 < J_1$).

In the antiferromagnetic phase II, two transitions as a function of temperature are also obtained for small values of J_2/J_1. However, the origin is different since the two phases involved here do not correspond to the same q value, and then they do not have the same T_N. Since, in Fig. 5, $T_N(q_1)$ and $T_N(q_2)$ were not obtained in the same approximation [three- and two-site mean field approximation, respectively, Eqs. (20) and (29)], it is interesting to compare both T_N in the same one-site approximation: in this case, for a second-order transition, T_N is given by the equation

$$k_B T_N(q) = \frac{-2J(q)}{2 + \exp[\Delta / T_N(q)]} \quad (34)$$

and $T_N(q_1) > T_N(q_2)$ if $|J(q_1)| > |J(q_2)|$, i.e., if $J_2/J_1 < \frac{1}{8}$. Thus in this case two transitions are obtained: the high-temperature phase being the mixed one VI, and the low-temperature phase being phase II. The critical value obtained by this simple calculation is very close to the one obtained in the elementary magnetic cell mean field approximation explained above, $J_2/J_1 = 0.15$.

On the other hand, the M-NM transition changes from second to first order as J_2 approaches the borderlines of phases VI and II with phase IX at $T = 0$ given by $J_2 = J_1/2 - \Delta/3$ and $J_2 = \Delta - J_1$, respectively (for $J_3 = 0$). This change of behavior also implies a sudden lowering of the critical temperature. This can also be explained using high-temperature expansion: near T_N, if the transition is second order, one has $m_q^2 = B(T_N - T)$ where B is positive. However, calculation of B shows that it becomes negative close to the borderline. Again in the one-site mean field approximation one obtains that B becomes negative if $\Delta/|J(q)| > (2 \ln 2)/3$.

Finally we would like to point out that Lee and Teitel in their calculation for the Coulomb interaction in the triangular lattice also obtain a second-order transition with increasing temperature between a nonmagnetic phase and a paramagnetic phase.[25] This Kosterlitz-Thouless transition is a property of two-dimensional lattices with long-range interactions. Although we have considered finite-range interactions, the nonmagnetic phase IX may have unusual behavior since at high temperature $\frac{2}{3}$ of the sites are magnetic. It will certainly be interesting to study this disordered phase.

VII. CONCLUSIONS

The effect of frustration on a system close to the M-NM instability allows one to understand the qualitative behavior of $R\mathrm{Mn}_2$ systems. For this case we have derived a model from the Hubbard Hamiltonian which contains these two ingredients. We have discussed other quite different physical situations that can be explained within the same picture.

The two methods used to study the effective Hamiltonian, Eq. (1), are complementary: the simulations allow one to find the stable configurations; the analytical method gives reliable results when the involved phases are compared. In spite of its simplicity the mean field calculation considering exactly the elementary magnetic cell gives very good agreement with the numerical results. This suggests that the method can also be useful for studying other frustrated structures, such as the fcc or the kagomé lattices.

Different kinds of magnetic orderings have been obtained, as observed in the $R\mathrm{Mn}_2$ compounds. In particular, the puzzling coexistence of magnetic and nonmagnetic sites can be explained and the recent observation of the predicted field-induced mixed phase on TbMn_2 (Ref. 28) seems to show the soundness of the proposed model. As we have commented, this mixed phase has also been experimentally observed as a function of pressure.[29]

In the triangular lattice we have stabilized mixed phases with only $\frac{1}{3}$ and $\frac{1}{9}$ nonmagnetic sites. The more complex structure of the $R\mathrm{Mn}_2$ compounds yields mixed phases with $\frac{1}{4}$ (ThMn_2) (Ref. 30) and $\frac{3}{4}$ (DyMn_2),[14] nonmagnetic sites. Preliminary Monte Carlo simulations show in fact that the effect of frustration is even more important in the real Laves phase structure: the stabilization of ordered structures with more nonmagnetic sites is expected.

On the other hand, such transitions where the number of magnetic sites changes imply large magneto-volume effects that must be taken into account in a more quantitative calculation. Interesting results have been recently obtained for TbMn_2: the transition from an AF to a mixed phase by the application of a field is accompanied by a 0.4% decrease in volume. The opposite occurs upon decreasing the field but it shows some hysteresis, as is frequently observed in these frustrated systems.[31]

There is no clear experimental example of the successive transitions with temperature. Two consecutive transitions, very close in temperature, are observed in TbMn_2 but further work is necessary to establish whether they are both due to magnetic transitions on the Mn sublattice or if the highest-temperature one involves the rare-earth atoms, Tb in this case.[10]

ACKNOWLEDGMENTS

We are indebted to E. Lelièvre for his help on the simulations. We thank R. Lemaire for pointing out the importance of this subject. The Laboratoire Louis Néel is associeé à l'Université Joseph Fourier.

*On leave from CONICET, Centro Atómico Bariloche, 8400 Bariloche, Argentina.

[1]A. P. Ramirez and R. N. Kleiman, J. Appl. Phys. **69**, 5252 (1991).

[2]J. T. Chalker, P. C. W. Holdsworth, and E. F. Shender, Phys. Rev. Lett. **68**, 855 (1992).

[3]For a recent review on frustrated systems, see P. Chandra and P. Coleman, in *Strongly Interacting Fermions and High T_c Superconductivity,* Proceedings of the Les Houches Summer School of Theoretical Physics, Les Houches, 1991, Session LVI, edited by J. Zinn-Justin and B. Douçot (North-Holland, Amsterdam, in press).

[4]R. Ballou, C. Lacroix, and M. D. Núñez-Regueiro, Phys. Rev. Lett. **66**, 1910 (1991); J. Magn. Magn. Mater. **104-107**, 753 (1992).

[5]M. Blume, Phys. Rev. **141**, 517 (1966).

[6]H. W. Capel, Physica **32**, 966 (1966).

[7]R. Ballou, J. Deportes, R. Lemaire, Y. Nakamura, and B. Ouladdiaf, J. Magn. Magn. Mater. **70**, 129 (1987).

[8]R. Ballou, J. Deportes, R. Lemaire, and B. Ouladdiaf, J. Appl. Phys. **63**, 3487 (1988).

[9]H. Wada, H. Nakamura, K. Yoshimura, M. Shiga, and Y. Nakamura, J. Magn. Magn. Mater. **70**, 134 (1987).

[10]R. Ballou, J. Deportes, R. Lemaire, P. Rouault, and J. L. Soubeyroux, J. Magn. Magn. Mater. **90-91**, 559 (1990).

[11]J. Voiron, R. Ballou, J. Deportes, R. M. Galera, and E. Lelievre, J. Appl. Phys. **69**, 5678 (1991).

[12]M. Shiga, J. Hirokawa, H. Wada, and Y. Nakamura, J. Phys. Soc. Jpn. **59**, 1410 (1990).

[13]K. Yoshimura, M. Shiga, and Y. Nakamura, J. Phys. Soc. Jpn. **55**, 3585 (1986).

[14]C. Ritter, S. H. Kilcoyne, and R. Cywinski, J. Phys. Condens. Matter **3**, 727 (1991).

[15]W. E. Evanson, J. R. Schrieffer, and S. Q. Wang, J. Appl. Phys. **41**, 1199 (1970); M. Cyrot, Phys. Rev. Lett. **25**, 871 (1970).

[16]E. N. Economou and P. Mihas, J. Phys. C **10**, 5017 (1977); T. Moriya and Y. Takahashi, J. Phys. Soc. Jpn. **45**, 397 (1978); J. Hubbard, Phys. Rev. B **19**, 2626 (1979); H. Hasegawa, J. Phys. Soc. Jpn. **46**, 1504 (1979); V. Heine, J. H. Samson, and C. M. M. Nex, J. Phys. F **11**, 2645 (1981).

[17]J. Friedel, in *The Physics of Metals,* edited by J. M. Ziman (Cambridge University Press, Cambridge, England, 1969), Vol. 1.

[18]G. Aeppli, A. Goldman, G. Shirane, E. Bucher, and M. C. Lux-Steiner, Phys. Rev. Lett. **58**, 808 (1987).

[19]C. Lacroix, J. Magn. Magn. Mater. **100**, 90 (1991).

[20]P. Haen, J. Flouquet, F. Lapierre, P. Lejay, and G. Remenyi, J. Low Temp. Phys. **67**, 391 (1987).

[21]J. Rossat-Mignod, P. Burlet, H. Bartholin, O. Vogt, and R. Lagnier, J. Phys. C **13**, 6381 (1980).

[22]J. A. Blanco, D. Gignoux, D. Schmitt, and C. Vettier, J. Magn. Magn. Mater. **97**, 4 (1991).

[23]J. A. Blanco, D. Gignoux, and D. Schmitt, Phys. Rev. B **45**, 2529 (1992).

[24]J. A. Blanco, D. Gignoux, J. C. Gómez-Sal, and D. Schmitt, J. Magn. Magn. Mater. **104-107**, 1273 (1992).

[25]Jong-Rim Lee and S. Teitel, Phys. Rev. Lett. **66**, 2100 (1991).

[26]R. M. F. Houtappel, Physica (Utrecht) **16**, 425 (1950).

[27]M. D. Núñez-Regueiro, C. Lacroix, R. Ballou, and E. Lelièvre, J. Magn. Magn. Mater. **104-107**, 285 (1992).

[28]R. Ballou, B. Ouladdiaf, P. J. Brown, M. D. Núñez-Regueiro, and C. Lacroix, Phys. Rev. B **45**, 3158 (1992).

[29]S. Mondal, R. Cywinski, S. H. Kilcoyne, B. D. Rainford, and C. Ritter, in Proceedings of the Internatinal Conference on Neutron Scattering, Oxford, 1991, [Physica B (to be published)].

[30]J. Deportes, R. Lemaire, B. Ouladdiaf, E. Roudaut, and F. Sayetat, J. Magn. Magn. Mater. **70**, 191 (1987).

[31]E. Lelièvre and R. Ballou (unpublished).

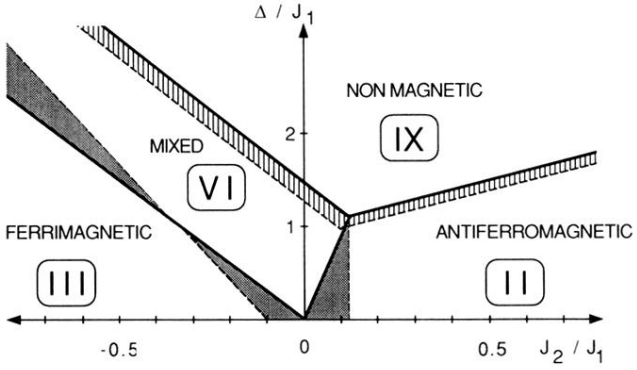

FIG. 5. Phase diagram for first- and second-neighbor interactions, $J_3=0$. The solid lines indicate the phase boundaries at $T=0$. The dashed lines separate regions with different temperature behavior: ▩ means that a first-order transition from the ground state to another ordered state is observed at $T_{N'}$, before reaching the nonmagnetic state at T_N; ▥ indicate regions where the transition at T_N is first order. In the other part of the diagram the transition to the nonmagnetic state at T_N is second order.